Molecular Biology of the Cell
Vol. 7, 1547–1558, October 1996

The Kinetochore Microtubule Minus-End Disassembly Associated with Poleward Flux Produces a Force that Can Do Work

Jennifer C. Waters,*† Timothy J. Mitchison,‡ Conly L. Rieder,§‖ and Edward D. Salmon*

*Department of Biology, University of North Carolina, Chapel Hill, North Carolina 27599-3280; ‡Department of Pharmacology, University of California at San Francisco, San Francisco, California 94143; §Division of Molecular Medicine, Wadsworth Center, New York State Department of Health, Albany, New York 12201-0509; and ‖Department of Biomedical Sciences, State University of New York, Albany, New York 12222

Submitted June 21, 1996; Accepted July 30, 1996
Monitoring Editor: J. Richard McIntosh

During metaphase and anaphase in newt lung cells, tubulin subunits within the kinetochore microtubule (kMT) lattice flux slowly poleward as kMTs depolymerize at their minus-ends within in the pole. Very little is known about how and where the force that moves the tubulin subunits poleward is generated and what function it serves during mitosis. We found that treatment with the drug taxol (10 μM) caused separated centrosomes in metaphase newt lung cells to move toward one another with an average velocity of 0.89 μm/min, until the interpolar distance was reduced by 22–62%. This taxol-induced spindle shortening occurred as kMTs between the chromosomes and the poles shortened. Photoactivation of fluorescent marks on kMTs revealed that taxol inhibited kinetochore microtubule assembly/disassembly at kinetochores, whereas minus-end MT disassembly continued at a rate typical of poleward flux in untreated metaphase cells. This poleward flux was strong enough to stretch the centromeric chromatin between sister kinetochores as much as it is stretched in control metaphase cells. In anaphase, taxol blocked kMT disassembly/assembly at the kinetochore whereas minus-end disassembly continued at a rate similar to flux in control cells (~0.2 μm/min). These results reveal that the mechanism for kMT poleward flux 1) is not dependent on kMT plus-end dynamics and 2) produces pulling forces capable of generating tension across the centromeres of bioriented chromosomes.

INTRODUCTION

To understand how chromosomes are segregated during mitosis, we must understand the forces that act on them. During prometaphase, opposing sister kinetochores on each chromosome must become attached to opposite spindle poles. Initially, one of the two sister kinetochores on a chromosome captures microtubules (MTs)[1] from one spindle pole. When the opposing sister kinetochore captures MTs from the other spindle pole, the now bioriented chromosome congresses to the spindle equator. While at the metaphase plate, sister kinetochores oscillate between constant velocity poleward (P) and away from the pole (AP) motility states. Various forces act on the chromosome while it interacts with the spindle. Kinetochore AP motion (Skibbens *et al.*, 1993) and polar microtubule ejection forces (reviewed in Fuller, 1995; Rieder and Salmon, 1995; Vernos and Karsenti, 1996) can push the chromatids toward the spindle equator. In addition, kinet-

† Corresponding author: Department of Biology, University of North Carolina, Chapel Hill, NC 27599-3280.

[1] Abbreviations used: kMTs, kinetochore microtubules; LM, light microscopy; MTs, microtubules.

ochore P motion (Skibbens *et al.*, 1993) and poleward flux of kMTs (Mitchison, 1989; Mitchison and Salmon, 1992) act to pull chromatids poleward.

In this report, we examine one of these forces: the poleward flux of tubulin subunits within the kMT lattice. This phenomenon was first predicted by the work of Forer (1965, 1966) and Margolis and Wilson (1981). It was later defined by Mitchison (1989), who observed a slow movement of subunits poleward when kMTs in metaphase PtK cells were marked by photoactivation of incorporated, caged-fluorescent subunits. KMT poleward flux has been found to occur during both metaphase and anaphase in mitotic newt lung cells (Mitchison and Salmon, 1992) and mammalian tissue cells (Mitchison, 1989; Zhai *et al.*, 1995), in vitro reconstituted *Xenopus* egg extract metaphase spindles (Sawin and Mitchison, 1991), and crane fly spermatocytes (Wilson *et al.*, 1994). During metaphase, net addition of tubulin subunits at the kMT plus-ends, which are attached to kinetochores in vivo, is balanced by persistent kMT minus-end depolymerization at the spindle pole. As a result, kMT subunits in newts move poleward with a velocity of ~0.5 μm/min (Mitchison and Salmon, 1992) while the kMTs remain approximately the same length. As anaphase is initiated, the incorporation of tubulin into kMT plus-ends ceases, and kinetochore poleward movement coupled to disassembly at kMT plus-ends predominates (Gorbsky *et al.*, 1987; Mitchison and Salmon, 1992; for insect spermatocytes, see Wilson *et al.*, 1994; Zhai *et al.*, 1995), resulting in kMT shortening and chromosome movement to the pole (i.e., anaphase A). During the initial stages of anaphase in newt lung cells, kMTs continue to depolymerize at their minus-ends, causing the lattice to flux poleward at a rate of 0.44 μm/min; within 4–5 min this rate decreases to 0.18 μm/min (Mitchison and Salmon, 1992).

During metaphase, kMTs remain a constant average length because flux is at a steady state of net MT plus-end polymerization and persistent minus-end depolymerization. Mitchison and Sawin (1990) predicted that inhibition of either of these parameters would result in useful work. However, it is not known where the force-generating mechanism for flux resides, nor has flux ever been shown to produce work outside of moving tubulin subunits.

One approach to better understanding spindle dynamics is to perturb MT polymerization or depolymerization with drugs. For example, Cassimeris and Salmon (1991) found that the drug nocodazole induces metaphase spindle shortening concurrent with kMT plus-end depolymerization at a rate of ~1.7-2 μm/min (for LLC-PK cells, see also Centonze and Borisy, 1991). As initially reported for PtK cells (DeBrabander *et al.*, 1986), we have found that the microtubule-stabilizing drug taxol (Schiff and Horwitz, 1980) also induces metaphase spindle shortening in newt lung cells, as their kMTs shorten at a rate of ~0.45 μm/min. In taxol-treated anaphase cells, the distance between the chromosomes and the pole also decreased, but at a rate of ~0.2 μm/min. The similarity in rates between taxol-induced kMT shortening and MT poleward flux led us to predict that low levels of taxol block MT assembly/disassembly dynamics at the kinetochore and that kMT shortening after taxol treatment is mediated solely by the kMT minus-end disassembly associated with poleward flux. To test this prediction, we used fluorescence photoactivation methods (Mitchison, 1989; Mitchison and Salmon, 1992). Our results demonstrate that, surprisingly, taxol arrests both growth and shortening of kMTs at the kinetochore attachment site. The disassembly of kMT minus-ends near the centrosome persists and generates pulling forces that result in work.

MATERIALS AND METHODS

Cell Culture

Primary newt (*Taricha granulosa*) lung cultures were established in Rose chambers, as described previously (Rieder and Hard, 1990; Waters *et al.*, 1993). Coverslips were subsequently mounted in a perfusion chamber and perfused during video light microscopy observation with 10 μM taxol prepared the day of the experiment from a 10 mM stock solution in dimethyl sulfoxide (DMSO) diluted with newt medium (consisting of 0.5× L-15 medium supplemented with 10% fetal calf serum, 10 mM HEPES, and antibiotics; Rieder and Hard, 1990). Control cells perfused with newt medium containing DMSO completed mitosis normally.

Video Light Microscopy (LM)

For video-enhanced differential interference contrast (VE-DIC) microscopy, cells were observed at 20–22°C with heat-filtered green light from a Nikon Microphot FX (Nikon, Garden City, NY) equipped with differential interference contrast (DIC) 60× (numerical aperture [NA] = 1.4) and 40× (NA = 0.85) objectives. Specimen illumination was shuttered between periods of observation and recording with a Uniblitz shutter controlled by an Image-1 (Universal Imaging, West Chester, PA) system. Video images were captured every 1–4 sec with a Hamamatsu C2400 video camera (Hamamatsu, Spring Branch, TX) and routed through Image-1 for processing. At this time the fixed noise and shading in the optical system were eliminated by background subtraction, and input images were averaged (16 frames) and contrast manipulated in real time. After processing, each image was stored on a Panasonic TQ 2028 optical memory disk recorder (ADCO Aerospace, Ft. Lauderdale, FL).

Immunofluorescence Microscopy

Cells followed by VE-DIC LM were fixed for tubulin immunolabeling by perfusion with glutaraldehyde and subsequently processed as described by Rieder and Alexander (1990). After the final wash, the chromosomes and nuclei were stained with Hoechst 33342 (0.02 mg/ml) in PBS for 5 sec. The processed coverslip cultures were then mounted on slides in PBS/glycerol, pH 7.8, containing *N*-propyl gallate. They were then examined with a Nikon Optiphot microscope equipped with a 60× (NA = 1.4) phase-contrast objective. Double-exposure color images were recorded on Fujichrome Velvia film (Fuji Photo Film, Tokyo, Japan), which was commercially processed. Black and white images were recorded on Ilford XP1 film with an ASA setting of 1600.

Cells were fixed and processed for 3F3/2 (Cyert *et al.*, 1988) labeling as described by Gorbsky and Ricketts (1993) and Waters *et al.* (1996). Cells were rinsed in PHEM (60 mM 1,4-piperazinediethanesulfonic acid [PIPES], 25 mM 4-(2-hydroxyethyl)-1-piperazine-ethanesulfonic acid [HEPES] at pH 7.0, 10 mM ethylene glycol bis(β-aminoethyl)ether-*N,N,N',N'*-tetra-acetic acid [EGTA], and 2 mM $MgCl_2$) and then simultaneously extracted and fixed in 0.5% Triton X-100, 0.5% formaldehyde, and 100 nM microcystin in PHEM for 5 min. The cells were then fixed further in 1.0% formaldehyde in PHEM for 15 min. After rinsing for 20 min in MBST consisting of 10 mM 3-(*N*-morpholino) propanesulfonic acid (MOPS) at pH 7.4 and 150 mM NaCl with 0.05% Tween 20, cells were blocked with 20% boiled goat serum in MBS (10 mM MOPS at pH 7.4 and 150 mM NaCl) and labeled for 45 min with an ascites preparation of 3F3/2 monoclonal antibody (a gift from Dr. G.J. Gorbsky, University of Virginia) diluted 1:1000 in 5% boiled goat serum in MBS. After being rinsed in MBST for 20 min, the cells were incubated for 30 min with a 1:200 dilution of TRITC-conjugated goat anti-mouse immunoglobulin G (IgG) in 5% boiled goat serum, rinsed for 20 min in MBST, and mounted in an antibleaching media (50% PBS and 50% glycerol containing *N*-propyl gallate). 3F3/2-labeled cells were viewed with a multimode digital fluorescence microscope system (Salmon *et al.*, 1994). A Nikon Microphot FX-A microscope equipped with a 60× (NA = 1.4) phase 4 objective was used. Images were captured with a Hamamatsu C4880-cooled CCD digital camera and routed to Metamorph image-processing software (Universal Imaging). The Metamorph software and a Ludl stepping motor were used to obtain Z-series optical sections of cells in 0.5-μm steps. Images were stored as stacks on optical disk cartridges with a Pinnacle Micro PMO-650 recorder.

Photoactivation and Vital Fluorescence Microscopy

Selected newt lung cells were microinjected, as described by Mitchison and Salmon (1992), with a mixture of 0.5 mg/ml rhodamine-labeled tubulin and 4.5 mg/ml C2CF tubulin in injection buffer (50 mM K-glutamate, 0.5 mM glutamic acid, and 0.5 mM $MgCl_2$). Coverslips containing injected cells were mounted in newt culture medium (see above) on glass-slide perfusion chambers.

Injected cells were photoactivated, and images were obtained with the multimode digital fluorescence microscope system (Salmon *et al.*, 1994) containing a Nikon Microphot FX equipped with phase and fluorescence optics with a Nikon PlanApo 60× objective (NA = 1.4). Phase images were collected by using green light shuttered between exposures. For fluorescence microscopy, Metamorph software (Universal Imaging) was used to control a Metaltek filter wheel. A shuttered HBO 100 W mercury lamp was used for fluorescence excitation and photoactivation. Digital images were collected with a Hamamatsu C4880 cooled-CCD camera and stored on a Pinnacle optical drive (Pinnacle Micro, Irvine, CA) for later analysis by Metamorph image analysis software. Fluorescent images were binned two times within the C4880 camera before transfer to the computer. This enhanced sensitivity 4× so that a two optical density (OD) filter could be used to decrease light intensity and prevent photobleaching.

Phase images were collected every 20 sec for at least 20 min after injection to ensure viability and to allow for incorporation of labeled tubulins into the spindle. At the appropriate stage of spindle formation, the culture medium within the chamber was replaced with new media containing 10 μM taxol. Phase and rhodamine images were then collected every 20 and 60 sec, respectively, until the taxol visibly took effect (3–5 min after taxol addition). A 25 μm × 3 mm slit (Melles Griot, Irvine CA), mounted on a Nikon pinhole slider, was then placed into the field diaphragm port in the epi-illumination pathway. A 1-sec exposure of 360-nm UV light was used to photoactivate a chosen region of the spindle. UV light removes the caging compound from the C2CF-labeled tubulin, thereby marking the spindle MTs by revealing the fluorophore. After photoactivation, phase images were collected every 20 sec and rhodamine and fluorescein images every 60 sec.

Data Analysis

From VE-DIC LM Records. After calibration in the X and Y axes with a Nikon stage micrometer, the particle tracking/analysis program within Image-1 was used to measure distances. X and Y pixel coordinates were recorded into memory and imported directly into Quattro Pro 4.0 (Borland International, Scotts Valley, CA) for calculations and graphing. For these analyses, sequential optical memory disk video images were routed into Image-1 through a time base corrector (For.A Corp, Natick, MA).

From Digital Fluorescence Records. Fluorescent digital images were analyzed with the tracking tools within Metamorph software. The system was calibrated as above, and distance measurements were imported directly into Microsoft Excel 5.0 (Microsoft, Redmond, WA) for calculations and graphing. Images were overlayed and pseudocolored by Adobe Photoshop 3.0 (Adobe Systems, Mountain View, CA) and then printed with a Tektronics Phaser IISDX dye-sublimation printer (Tektronics, Wilsonville, OR). Interkinetochore distances were measured from z-series stacks, as described (Waters *et al.*, 1996).

RESULTS

Taxol Induces Late Prometaphase/Metaphase Spindles to Shorten

As previously reported by DeBrabander and coworkers (1986) for PtK cells, we found that 10 μM taxol induced the centrosomes in late prometaphase/metaphase newt lung cells to move toward the chromosomes. This taxol-induced spindle shortening occurred only in cells that contained bipolarly attached chromosomes (our unpublished observations). We perfused nine late prometaphase/metaphase newt lung cells with 10 μM taxol (Figure 1). After drug treatment (3–5 min), the distance between the centrosomes began to decrease with an average velocity of 0.89 μm/min (range, 0.61–1.3 μm/min; n = 9). This motion continued until the interpolar distance was reduced by 22–62%. Subsequent immunofluorescence analyses of these cells revealed that the spindles consisted of two dense half-spindle/astral MT arrays, with the longest MTs extending ~12 μm (Figure 1f).

Analyses of DIC and phase-contrast video records also revealed that the oscillatory motions characteristically exhibited by mono- and bioriented chromosomes in prometaphase and metaphase newt lung cells (Skibbens *et al.*, 1993) became arrested within 5 min of taxol addition (our unpublished results; for monopolar spindles, see also Ault *et al.*, 1991). Meanwhile, the normal saltatory motion of particles along the astral microtubules continued (our unpublished results).

During Metaphase, Taxol Inhibits Assembly and Disassembly of KMT Plus-Ends at the Kinetochores but not Disassembly of Minus-Ends at the Poles

We used photoactivation methods to determine whether the taxol-induced shortening of kMTs we observed in metaphase cells occurs by depolymerization of kMTs at their plus-ends in the kinetochore

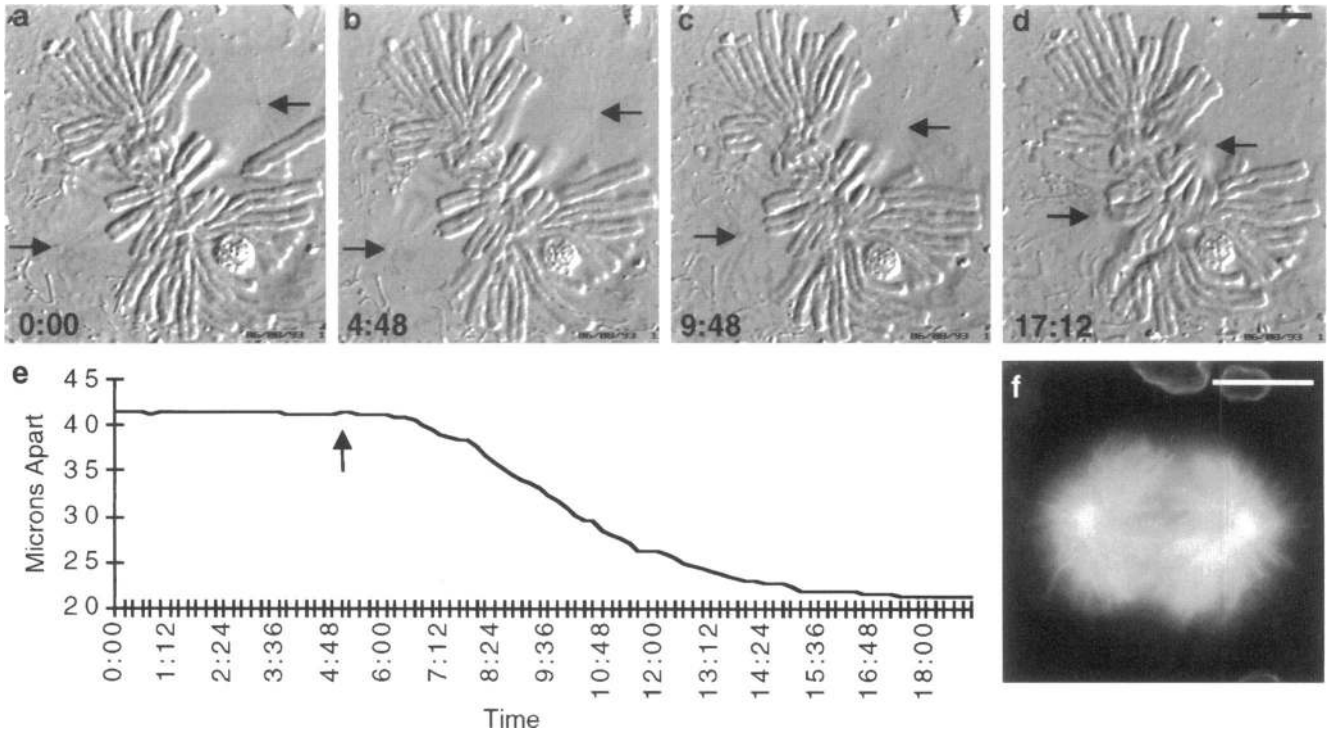

Figure 1. Video micrographs of centrosome behavior during metaphase (arrows) before (a and b) and after (c and d) 10 μM taxol treatment. Elapsed time is shown in min:sec. (e) Distance between centrosomes in the cell shown in a–d. Arrow notes when taxol was added. (f) Immunofluorescence distribution of MTs in a metaphase cell shortly after taxol treatment. Taxol induces centrosomes in cells with bipolarly attached chromosomes to move toward one another over 10–15 min with an average initial velocity of ~0.89 μm/min. Bar in d, 10 μm; bar in f, 20 μm.

and/or at their minus-ends in the pole. We microinjected caged fluorescein-labeled (C2CF) tubulin and rhodamine-labeled tubulin into late prometaphase/metaphase newt lung cells. After waiting at least 20 min for the labeled tubulins to incorporate into the spindles (Mitchison and Salmon, 1992), we treated the cells with 10 μM taxol. Once the spindles began to shorten (3–5 min), we locally marked MTs by irradiating (with 360-nm light) a thin bar-shaped region across the spindle to photoactivate the C2CF-labeled tubulin (Figure 2, time 5:44). These marks, which could be clearly discerned on the kMT bundles, were used as reference points to determine where depolymerization of kMTs was taking place during taxol-induced spindle shortening.

These experiments revealed that, as the kMTs shortened in response to taxol, the distance between the kinetochores and the photoactivated marks remained constant (Figures 2, time 5:44–25:44, and 3). Meanwhile, the pole moved toward the fluorescent marks with an average velocity of 0.43 μm/min (n = 4; range, 0.29–0.50 μm/min; Figures 2, time 5:44–25:44, and 3). The kMT bundles remained distinct throughout the shortening process (Figure 2). In control cells, the pole-to-pole distance did not change significantly as the photoactivated marks moved toward the poles at an average rate of 0.58 μm/min (n = 5; range, 0.43–0.85 μm/min; Figure 2). Our control value is similar to the 0.54 μm/min average rate of MT poleward flux previously determined by Mitchison and Salmon (1992) for metaphase newt lung cells.

During Anaphase, Taxol Inhibits Plus-End but not Minus-End Disassembly

During anaphase in newt lung cells, kMTs shorten because of both rapid disassembly at their plus-ends within the kinetochore and slow disassembly at their minus-ends within the pole (Mitchison and Salmon, 1992; Zhai *et al.*, 1995). This was evident in our control cells; kinetochores moved toward and "consumed" the photoactivated mark as the mark moved slowly poleward (Figure 4; see also Gorbsky *et al.*, 1987; Mitchison and Salmon, 1992). Mitchison and Salmon (1992) found that the disassembly of kMT minus-ends slows during anaphase in newt cells; flux occurs at 0.44 μm/min in the first few minutes of anaphase and 0.18 μm/min ~4-5 min after anaphase onset. We reasoned that if the kMT minus-end disassembly that occurs in taxol-treated metaphase cells is due to pole-

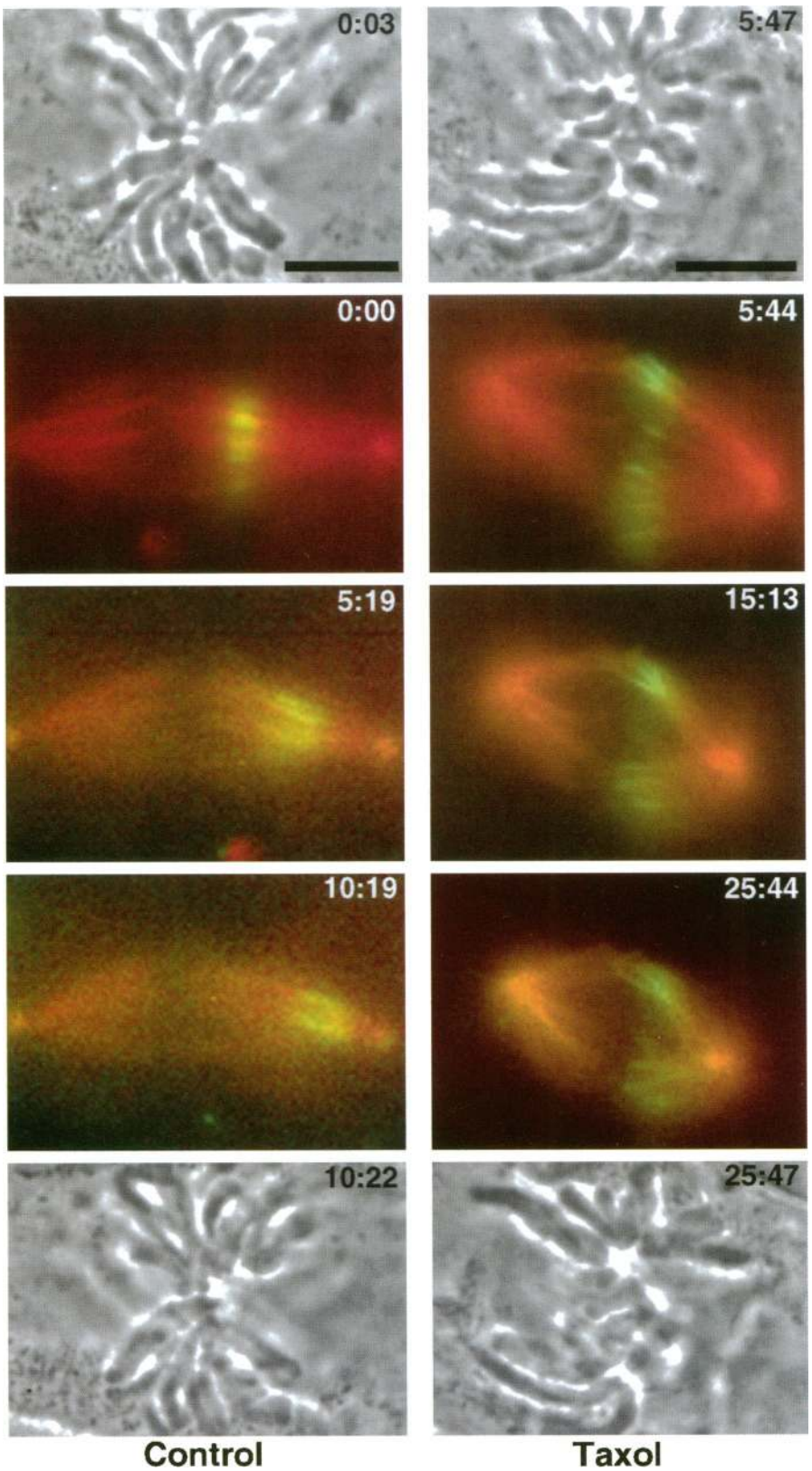

Figure 2. Photoactivation marking of a control (left panel) and a taxol-treated (right panel) metaphase cell. Images on the left were taken from one control cell over time; images on the right were taken from one taxol-treated cell over time. Time is shown in min:sec elapsed (after 10 μM taxol addition for taxol-treated cell). 0:03, 10:22, 5:47, and 25:47 are phase contrast images showing congressed chromosomes. 0:00 and 5:44 are overlays of rhodamine and fluorescein tubulin images within 5 sec of photoactivation. In control cells, net addition of MT subunits at the kinetochore and loss of subunits at the pole cause the photoactivated mark to move poleward (0:00–10:19). As taxol induces slow K-fiber shortening, marks at the kinetochore remain stationary relative to the chromosomes while the pole moves toward the mark and the chromosomes (5:44–25:44). This demonstrates that taxol inhibits MT assembly/disassembly at the kinetochore, whereas MT loss at the pole continues. Persistent spindle microtubule turnover and enhanced assembly throughout the shortening process result in a gradual change in the spindle color from red to orange in these pseudocolored overlays. Note that background fluorescence in microinjected cells is high, compared with fixed and extracted cells (Figure 1f), because of unincorporated labeled tubulin. These fluorescence images were contrast enhanced so that kinetochore fibers are clearly visible, and this obscures the visualization of the astral microtubules that are seen in Figure 1f.

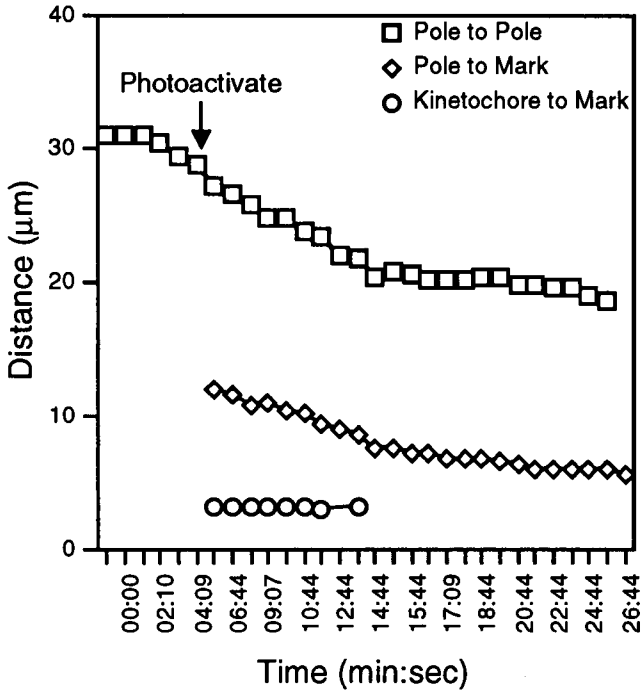

Figure 3. Graph of measurements from the photoactivated taxol-treated metaphase cell shown in Figure 2. Taxol was added at 0:00. Squares plot distance between the spindle poles over time. Taxol induced the poles in this cell to move together at a rate of 0.63 μm/min (average = 0.89 μm/min). Diamonds plot distance between the spindle pole and the photoactivated mark over time. In this cell, the pole moves toward the mark at a rate of 0.29 μm/min (average = 0.43 μm/min). Circles plot the distance between the mark and a kinetochore, which remains constant over time.

ward flux, then it should slow down in anaphase, as is seen in control anaphase cells.

Because it takes 3–5 min for taxol to take effect and metaphase newt lung cells treated with taxol only rarely progress to anaphase (our unpublished observation), it was not possible to reliably determine the effect of taxol on the first 5 min of anaphase A when kinetochore motility and flux is maximum. However, by perfusing cells immediately after chromatid separation, we could evaluate the effect of taxol ~5 min into anaphase when kMT disassembly at the pole is occurring at ~0.18 μm/min in control newt cells (Mitchison and Salmon, 1992). We photoactivated five taxol-treated anaphase cells (Figures 4 and 5). In one cell, no chromosome-to-pole shortening occurred. It is likely that flux had stopped in this cell (as is often seen in controls; Mitchison and Salmon, 1992) before taxol had taken effect. In four cells, the distance between the chromosomes and the pole decreased at an average rate of 0.2 μm/min (range, 0.14–0.27 μm/min). In these cells, the distance between the photoactivated mark and the pole decreased at the same average rate, 0.2 μm/min (range, 0.14–0.24 μm/min; Figures 4, time 6:09–12:29, and 5), a rate similar to that of flux in control cells during anaphase (0.18 μm/min; Mitchison and Salmon, 1992).

Kinetochore Microtubule Poleward Flux Generates Tension across the Centromeres of Bioriented Chromosomes

To determine whether the forces for taxol-induced spindle shortening act on the kMTs and stretch the centromeres, we measured the distance between kinetochores in taxol-treated cells. We filmed four late prometaphase/metaphase cells treated with 10 μM taxol and fixed them while their spindles were actively shortening (5–8 min after taxol addition). We then processed the cells for immunofluorescence labeling with the monoclonal antibody 3F3/2 (Figure 6A). In newt lung cells, 3F3/2 labels centrosomes, the surface of the chromosomes, and kinetochores uniformly throughout mitosis (Figure 6A; Waters *et al.*, 1996). Z-axis optical serial sections (0.5-μm steps) through labeled cells were collected as 12-bit images by a cooled CCD camera and transferred to Metamorph software. 3F3/2 chromosome labeling allowed identification of individual chromosomes within the three-dimensional stacks and, therefore, sister kinetochores. On the basis of the measurements made from 38 sister kinetochore pairs in four spindles shortening in response to taxol, the average interkinetochore distance was 1.8 ± 0.47 μm (range, 1.1–2.8; Figure 6B and Table 1). Because the average interkinetochore rest length (i.e., the distance between kinetochores on a chromosome that is not interacting with microtubules) in newts is 1.1 μm (Waters *et al.*, 1996), the centromeres in cells treated with taxol for 5–8 min are stretched (Table 1). After 30 min in taxol, we found that the spindles had stopped shortening. We measured the distance between kinetochores on bioriented chromosomes that had been treated with taxol for >30 min and found that the centromeres were only minimally stretched (average = 1.2 μm ± 0.1; range, 1.0–1.4 μm; n = 11 from 2 cells; Table 1).

DISCUSSION

Kinetochore Microtubule Plus- and Minus-End Dynamics Are Differentially Sensitive to Taxol

Our results reveal that 10 μM taxol preferentially inhibit kMT assembly/disassembly at their plus-ends without inhibiting the disassembly at their minus-ends in the spindle pole (Figure 7B). This has two observable consequences for the metaphase spindle. First, presumably because the characteristic oscillations of kinetochores depend on normal MT plus-end dynamics at the kinetochores (Ault *et al.*, 1991; Skibbens *et al.*, 1993), taxol rapidly arrests chromosome oscillations at all stages of mitosis (our observa-

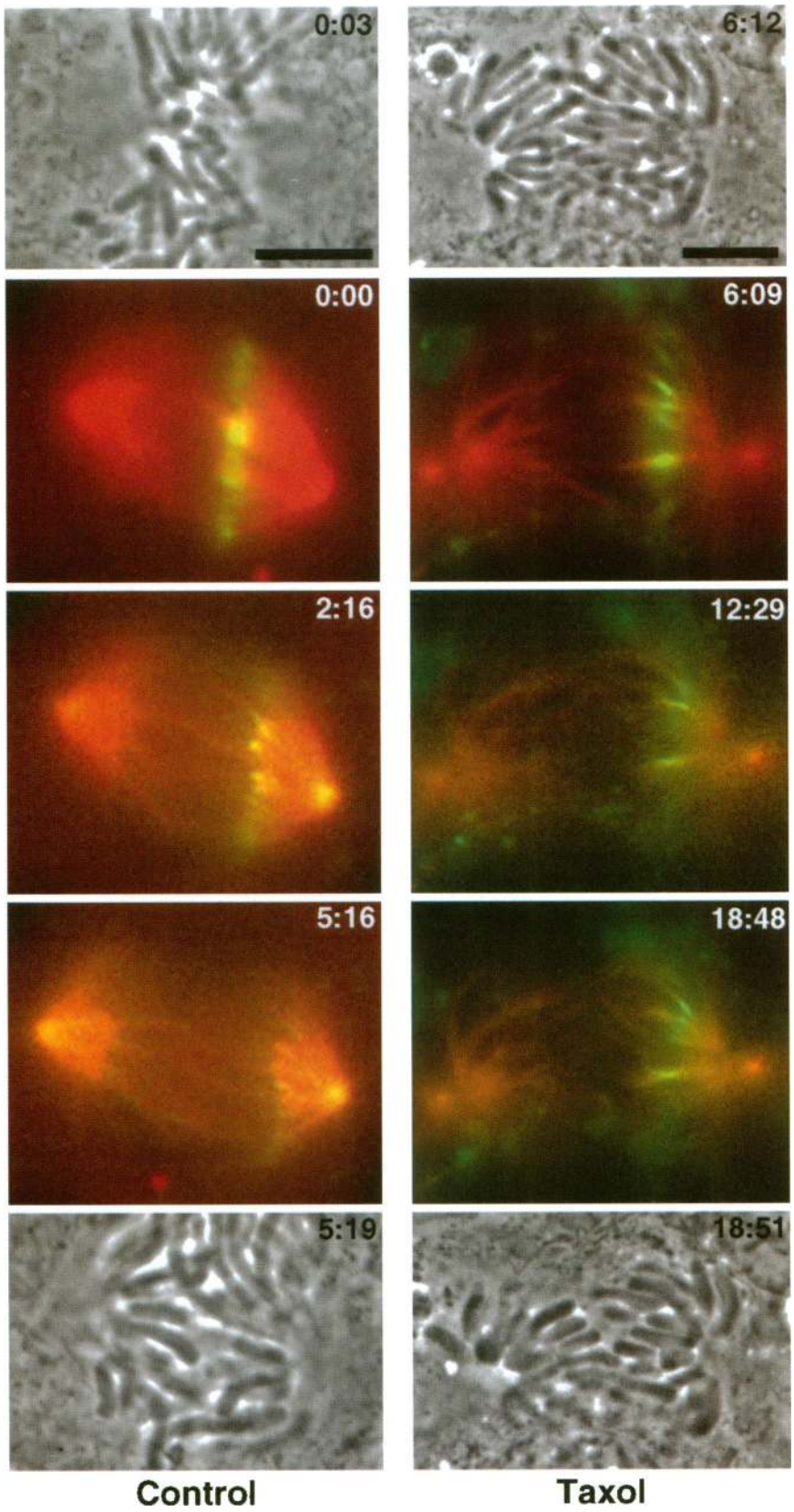

Figure 4. Photoactivation marking of a control and a taxol-treated anaphase cell. Images on the left were taken from one control cell over time; images on the right were taken from one taxol-treated cell over time. Time is shown in min:sec elapsed (after 10 μM taxol addition for taxol-treated cell). 0:03, 6:09, 5:19, and 18:51 are phase contrast images showing chromosome distribution. 0:00 and 6:09 are overlays of rhodamine and fluorescein tubulin images within 5 sec of photoactivation. In control cells, kMTs disassembled rapidly at their plus-ends within the kinetochore and slowly at their minus-ends within the pole, resulting in chromosome-to-pole movement (i.e., anaphase A). Loss of tubulin subunits at the plus-end of the kMT caused the distance between the kinetochore and the photoactivated mark to continuously decrease (0:00, 2:16), eventually leading to complete loss of photoactivated subunits comprising the mark (5:16). Meanwhile, poles separated to elongate the spindle (i.e., anaphase B; 0:00–5:16). In taxol-treated cells, the distance between the kinetochore and the pole decreased at the same slow rate as the distance between the mark and the pole (see graph in Figure 5). This demonstrates that taxol inhibits the rapid kinetochore-mediated plus-end disassembly that occurs during anaphase, while slow depolymerization of kMTs at the minus-end continues (6:09–18:48). Taxol also inhibited anaphase B (6:09–18:48).

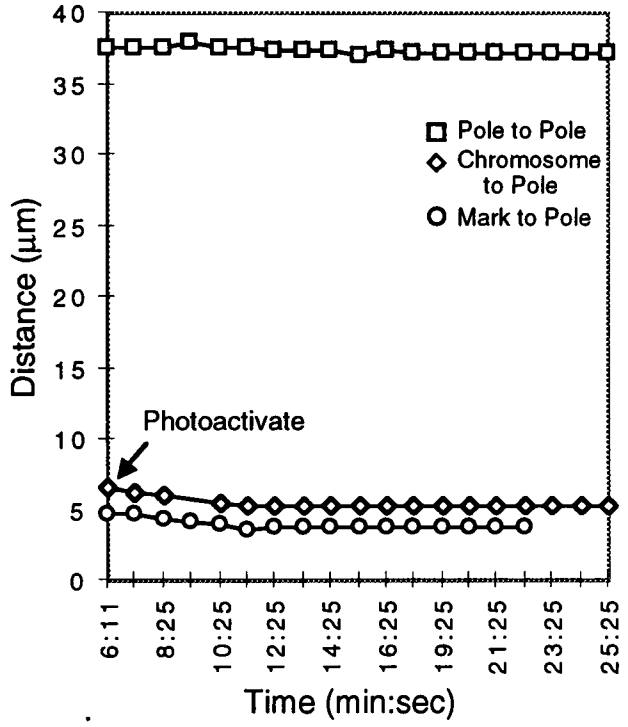

Figure 5. Graph of measurements from the photoactivated taxol-treated anaphase cell shown in Figure 4. Taxol was added at 0:00. Squares plot distance between the spindle poles, which remains constant over time. Diamonds plot distance between the spindle pole and a chromosome over time. In this cell, the K-fiber shortened at a rate of 0.27 μm/min. Circles plot the distance between the mark and the pole, which decreased at a rate of 0.24 μm/min.

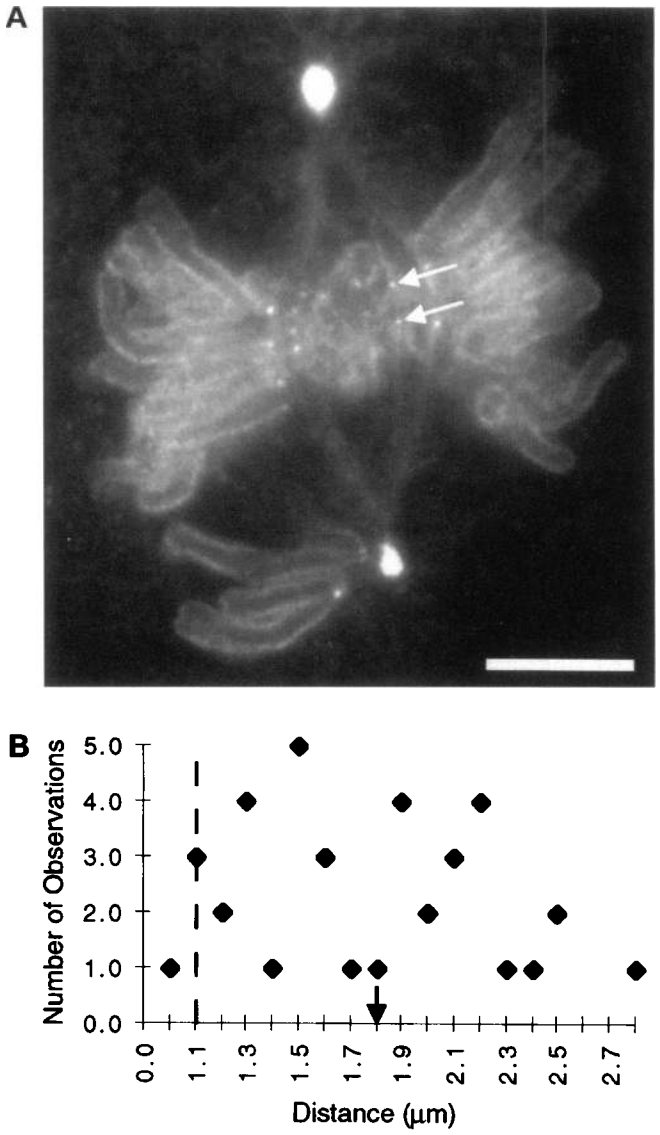

Figure 6. Analysis of interkinetochore distances for bioriented chromosomes in taxol-treated newt lung cells by indirect immunofluorescence. (A) Immunofluorescence micrograph obtained by using the 3F3/2 antibody shows the brightly labeled kinetochores and the weakly labeled surface of the chromatin. Each kinetochore (white arrows) in one sister kinetochore pair is labeled. Single dots (no arrows) are kinetochores whose sisters are in a different focal plane. Bar, 10 μm. (B) Histogram of interkinetochore distances for 38 taxol-treated bioriented chromosomes obtained from image stacks of four immunolabeled cells, plotted against frequency of occurrence. Dashed vertical line indicates interkinetochore rest length (1.1 μm) for comparison. Arrow indicates the average value (1.8 μm) for the data set.

tions; see also Ault *et al.*, 1991). Second, the kMTs shorten and the poles move toward the kinetochores that are positioned near the spindle equator (Figure 7, A and B). The average rate of kinetochore-to-pole movement (0.43 μm/min), which we show to be coupled to the disassembly of kMTs at their minus-ends within the pole, is similar to the rate at which MT subunits are normally lost at the pole because of flux (average = 0.58 μm/min). Importantly, the rate at which kMTs shorten after taxol addition decreases in anaphase cells (0.2 μm/min) to the rate at which flux occurs in control anaphase cells (0.18 μm/min; Mitchison and Salmon, 1992). From these data we conclude that kMT shortening in response to taxol is not the result of taxol actively inducing kMT minus-end disassembly. Rather, in the presence of taxol, the kMT minus-end disassembly that occurs in control cells caused by the flux mechanism persists (Figure 7, A and B), whereas plus-end dynamics at the kinetochore are inhibited.

In taxol-treated metaphase cells the poles move toward one another until the distance between them is reduced, on average, to 22–62% of the original interpolar distance. Why doesn't minus-end disassembly of kMTs in the pole continue until the kMTs no longer exist? Recent work on the effects of taxol on MTs grown in vitro reveals that low concentrations of taxol selectively suppress the shortening of MT plus-ends but that high levels completely suppress the dynamic

Table 1. Interkinetochore distances

	Average (μm)	Range
Rest length[a]	1.1	0.9–1.3
Control metaphase[a]	1.8	1.0–2.4
Metaphase, 5–8 min after taxol addition	1.8	1.1–2.8
Metaphase, 30 min after taxol addition	1.2	1.0–1.4

[a] Taken from Waters *et al.*, 1996.

behavior of both MT ends (Derry *et al.*, 1995). Although the kinetics of taxol uptake by newt lung cells are unknown, it is likely that the intercellular concentration of this drug progressively increases during our 20–30 min treatment period. Thus, it is possible that the initial concentration of the drug in the cell is low and preferentially disrupts plus-end MT dynamics without affecting the normal behavior of MT minus-ends. Then, as the drug accumulates over time, activity at the MT minus-ends also becomes suppressed. This is supported by our finding that the centromeres in taxol-treated cells are no longer stretched once the spindle has stopped shortening (Table 1).

Poleward Kinetochore Microtubule Flux Produces a Force that Can Move Centrosomes and Stretch Centromeres

During taxol-induced spindle shortening, the spindle poles move toward the chromosomes at the same rate that the kMTs are disassembled at the poles by the flux mechanism (Figure 7, A and B). Taxol-induced spindle shortening only occurs in cells that contain bioriented chromosomes. This suggests that taxol-induced spindle shortening is dependent on kMT minus-end disassembly (i.e., the flux mechanism). We have also shown that centromeres are stretched during taxol-induced spindle shortening. After spindle shortening ceases, the centromeres are no longer stretched. Other forces that may be present and could cause taxol-induced spindle shortening, such as pulling forces generated by antiparallel MTs interacting in the spindle midzone or pushing forces generated by astral MTs, would not act on the kMTs and would not stretch the centromeres. Therefore, flux-mediated minus-end disassembly of kMTs is the dominant force that pulls the spindle poles together.

Implications for the Mechanism of Flux

Several models describe how the force that produces flux may be generated (Sawin and Mitchison, 1994). Our data demonstrate that the force that produces flux is capable of moving centrosomes and stretching centromeric chromatin. Therefore, the mechanism by which flux is generated must meet the following criteria: 1) it must produce a force in a manner that is not dependent on plus-end dynamics; 2) it must be able to hold onto depolymerizing MT minus-ends while linking them to the centrosome; and 3) it must promote MT minus-end disassembly. We favor a model proposing the existence of an "MT minus-end capping complex" (Figure 7, C and D; see also Sawin and Mitchison, 1994). In this model, the MT minus-ends are capped with a sleeve-like complex that attaches to the MT lattice (Figure 7D). This complex could be part of the γ-tubulin complex (Moritz *et al.*, 1995; Zheng *et al.*, 1995). The association between the minus-end complex and the MT lattice may involve MT motor proteins that produce a force that pulls the MT into the sleeve. Thermodynamic energy from MT depolymerization (Maekawa *et al.*, 1991; Desai and Mitchison, 1995; Inoue and Salmon, 1995) may contribute to force generation. However, we have found that taxol, a drug that has a stabilizing effect on MTs (Schiff and Horwitz, 1980) and thus reduces the energy available from depolymerization, does not affect the velocity of flux. Therefore, it is more likely that MT disassembly within the minus-end complex is mediated by an MT-severing protein like katanin (McNally and Vale, 1993), or an MT motor like Kar3, which has been shown to induce the disassembly of taxol-stabilized MT minus-ends in vitro (Endow *et al.*, 1994b). Proteins like NuMA (Gaglio *et al.*, 1995) or homologues of the minus-end MT motor Ncd (Endow *et al.*, 1994a) may help to maintain spindle pole organization as subunits are lost at the MT minus-end (Figure 7C).

Implications for the Role of Flux

The role of kMT poleward flux in mitosis is unknown. The poleward movement of kMTs clearly contributes to poleward kinetochore motion during oscillations and anaphase A. In egg extracts (Sawin and Mitchison, 1991) and spermatocytes (Wilson *et al.*, 1994), flux may account for the majority of anaphase A. However, during anaphase in somatic cells, the majority of chromosome-to-pole movement occurs concurrent with depolymerization of the kMTs at the kinetochore (63% in newt, Mitchison and Salmon, 1992; 84% in PtK, Zhai *et al.*, 1995). In addition, flux slows significantly during anaphase in newt lung cells and slows abruptly at anaphase onset in PtK cells. It is possible that, in somatic cells, kMT poleward flux is a consequence of the dynamic organization of spindles and does not have an actual function in mitosis. However, our data show that during metaphase the poleward flux mechanism generates forces that produce work and stretch the centromeres of chromosomes as much as occurs in control cells when kinetochores are dynamic. Therefore, we believe that, in somatic cells, kMT poleward

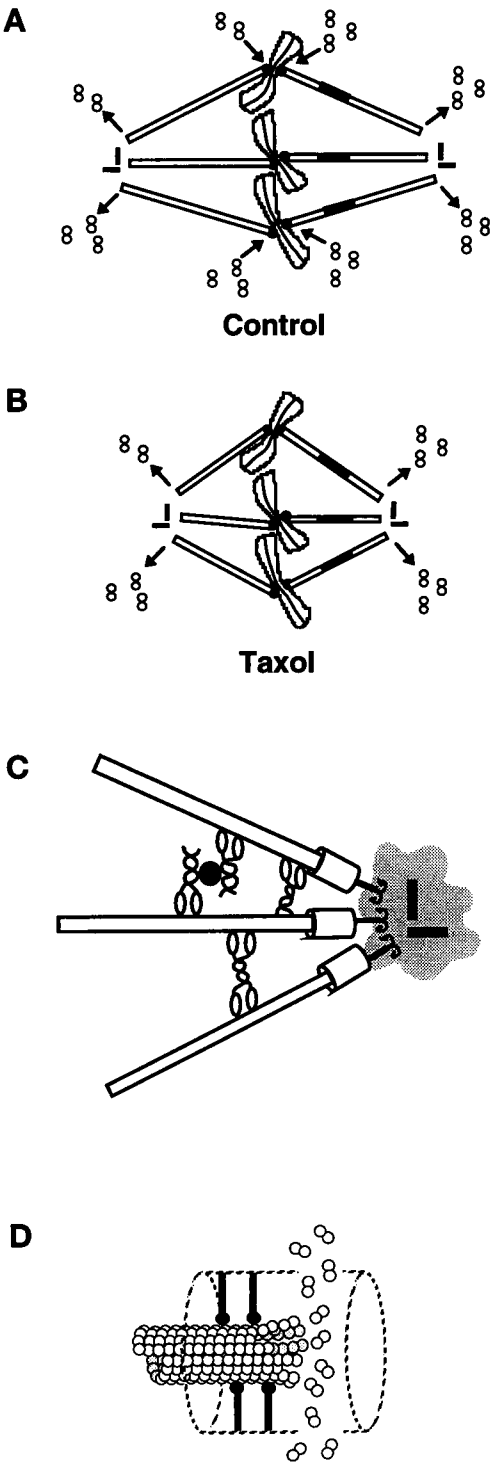

Figure 7. (A and B) A diagram summarizing the effect of taxol on kMT ends. Black bars on microtubules represent photoactivated marks. (A) In control cells, subunit loss at the pole is balanced by net subunit addition at the kinetochore. (B) Taxol inhibits MT assembly/disassembly exchange at the kinetochore but does not inhibit subunit loss at the pole. This results in shorter kMTs and a decrease in the distance between spindle poles. (C and D) A model of the

flux plays an important role primarily before anaphase onset.

Micromanipulation experiments have shown that tension across centromeric chromatin can stabilize kinetochore attachment to microtubules (Nicklas and Koch, 1969), change the direction of kinetochore motility (Nicklas, 1977; McNeill and Berns, 1981; Rieder *et al.*, 1986; Hays and Salmon, 1990; Ault *et al.*, 1991), and regulate cell-cycle progression (see also McIntosh, 1991; Gorbsky, 1995; Nicklas *et al.*, 1995; Wells, 1996). In vivo, tension across the centromere has been proposed to be generated as poleward forces on the kinetochore (which are produced by poleward flux and kinetochore P motility) are resisted by sister kinetochore P motility toward opposite poles, as well as ejection forces acting to push the chromosome arms away from the pole. We have recently shown that, while newt sister kinetochores are oscillating between P and AP movement, they are, on average, under tension (Waters *et al.*, 1996). We demonstrate here that kMT poleward flux alone produces enough force to stretch centromeres to the same extent they are stretched in control metaphase cells (Table 1). Therefore, it may be that the primary role of kMT poleward flux in newt lung cells is to ensure that oscillating kinetochores are under net tension.

The current model is that kinetochores switch to AP motion at high tension and to P motion at low tension (Skibbens *et al.*, 1993, 1995; Cassimeris *et al.*, 1994; Rieder and Salmon, 1995). According to this model, sister kinetochores generate tension across the centromere on their own. Why then should they need the help of flux? If tension plays a key role in the direction of kinetochore motility, kinetochore attachment, and a checkpoint control for anaphase onset, it is truly important to mitosis. Therefore, it is not unlikely that the cell has evolved redundant mechanisms for generating tension across the centromere. In addition, when kinetochores move AP, tension across the centromere is relieved, and sometimes the centromere becomes compressed (Skibbens *et al.*, 1993; Waters *et al.*, 1996). KMT poleward flux provides a constant poleward force that may be necessary in maintaining the tension at the kinetochore needed for stabilization of MT attachment and proper orientation of sister kinetochores to opposing spindle poles (Nicklas and Koch, 1969; Ault and Nicklas, 1989). These results raise an interesting question: what are the relative strengths of kinetochore-pulling forces and poleward kMT flux forces? Our results indicate that, at the very least, they

(Figure 7 cont.) "minus-end complex." (C) In this model, MT minus-ends are capped with a minus-end complex, which is anchored to the pericentriolar material. Minus-end MT motor proteins or proteins such as NuMA (Gaglio *et al.*, 1995) may help to maintain spindle pole organization. (D) The minus-end capping complex holds onto the MT lattice while the MT depolymerizes.

are comparable in strength. However, flux could be much stronger. The idea that fast weaker kinetochore forces coexist with slow stronger flux forces is very important for the mechanism of prometaphase congression, anaphase segregation of chromosomes, and the spindle assembly checkpoint. For example, it could be that kinetochore motility itself is insufficient to overcome the checkpoint sensor of tension, and the stronger pulling by the flux machinery is required.

In control cells, the sister kinetochores on properly bioriented chromosomes are under net tension (Waters *et al.*, 1996). This tension has been proposed to comprise part of the spindle assembly checkpoint for anaphase onset that regulates when a cell exits mitosis and enters interphase (reviewed in McIntosh, 1991; Gorbsky, 1995; Wells, 1996). Our results show that after 30 min in taxol kMT minus-end disassembly stops resulting in the loss of tension across the centromere. Therefore, taxol may arrest cells in metaphase (Jordan *et al.*, 1993; Rieder *et al.*, 1994) because it eventually inhibits the generation of tension between sister kinetochores.

ACKNOWLEDGMENTS

This paper is dedicated to the memory of J.C.W.'s father, Louis W. Waters (1938–1994). We thank Arshad Desai (University of California at San Francisco, CA) for preparing C2CF-labeled tubulin and teaching J.C.W. how to prepare C2CF-labeled tubulin, Dr. Steve Parsons (University of North Carolina, Chapel Hill, NC) for preparing the rhodamine-labeled tubulin, Richard Cole (Wadsworth Center, Albany, NY) for his assistance during the early stages of this study, Dr. Bob Skibbens (Johns Hopkins, Baltimore, MD) for teaching J.C.W. how to microinject cells, and Paul Maddox (University of North Carolina, Chapel Hill, NC) for excellent technical assistance. This work was supported, in part, by National Institutes of Health grants GM-24364 to E.D.S, GM-40198 to C.L.R., and GM-29565 to T.J.M.

REFERENCES

Ault, J.G., Demarco, A.J., Salmon, E.D., and Rieder, C.L. (1991). Studies on the ejection properties of asters: astral microtubule turnover influences the oscillatory behavior and positioning of monooriented chromosomes. J. Cell Sci. *99*, 701–710.

Ault, J.G., and Nicklas, R.B. (1989). Tension, microtubule arrangements, and the proper distribution of chromosomes in mitosis. Chromosoma *98*, 33–39.

Cassimeris, L., Rieder, C.L., and Salmon, E.D. (1994). Microtubule assembly and kinetochore directional instability in vertebrate monopolar spindles: implications for the mechanism of chromosome congression. J. Cell Sci. *107*, 285–297.

Cassimeris, L., and Salmon, E.D. (1991). Kinetochore microtubules shorten by loss of subunits at the kinetochores of prometaphase chromosomes. J. Cell Sci. *98*, 151–158.

Centonze, V.E., and Borisy, G.G. (1991). Pole-to-chromosome movements induced at metaphase: sites of microtubule disassembly. J. Cell Sci. *100*, 205–211.

Cyert, M.S., Scherson, T., and Kirschner, M.W. (1988). Monoclonal antibodies specific for thiophosphorylated proteins recognize *Xenopus* MPF. Dev. Biol. *129*, 209–216.

DeBrabander, M., Geuens, G., Nuydens, R., Willebrords, R., Aerts, F., and DeMey, J. (1986). Microtubule dynamics during the cell cycle: the effects of taxol and nocodazole on the microtubule system of PtK2 cells at different stages of the mitotic cycle. Int. Rev. Cytol. *101*, 215–274.

Derry, W.B., Wilson, L., and Jordan, M.A. (1995). Substoichiometric binding of taxol suppresses microtubule dynamics. Biochemistry *34*, 2203–2211.

Desai, A., and Mitchison, T.J. (1995). A new role for motor proteins as couplers to depolymerizing microtubules. J. Cell Biol. *128*, 1–4.

Endow, S.A., Chandra, R., Komma, D.J., Yamamoto, A.H., and Salmon, E.D. (1994a). Mutants of the *Drosophila* ncd microtubule motor protein cause centrosomal and spindle pole defects in mitosis. J. Cell Sci. *107*, 859–867.

Endow, S.A., Kang, S.J., Satterwhite, L.L., Rose, M.D., Skeen, V.P., and Salmon, E.D. (1994b). Yeast Kar3 is a minus-end microtubule motor protein that destabilizes microtubules preferentially at the minus-ends. EMBO J. *13*, 2708–2713.

Forer, A. (1965). Local reduction of spindle birefringence in living *Nephrotoma suturalis* (Loew) spermatocytes induced by ultraviolet microbeam irradiation. J. Cell Biol. *25*, 95–117.

Forer, A. (1966). Characterization of the mitotic traction system, and evidence that birefringent spindle fibers neither produce nor transmit force for chromosome movement. Chromosoma *19*, 44–98.

Fuller, M.T. (1995). Riding the polar winds: chromosomes motor down east. Cell *81*, 5–8.

Gaglio, T., Saredi, A., and Compton, D.A. (1995). NuMA is required for the organization of microtubules into aster-like mitotic arrays. J. Cell Biol. *131*, 693–708.

Gorbsky, G.J. (1995). Kinetochores, microtubules, and the metaphase checkpoint. Trends Cell Biol. *5*, 143–148.

Gorbsky, G.H., and Ricketts, W.A. (1993). Differential expression of a phosphoepitope at the kinetochores of moving chromosomes. J. Cell Biol. *122*, 1311–1321.

Gorbsky, G.J., Sammak, P.J., and Borisy, G.G. (1987). Chromosomes move poleward in anaphase along stationary microtubules that coordinately disassemble from their kinetochore ends. J. Cell Biol. *104*, 9–18.

Hays, T.S., and Salmon, E.D. (1990). Poleward force at the kinetochore in metaphase depends on the number of kinetochore microtubules. J. Cell Biol. *110*, 391–404.

Inoue, S., and Salmon, E.D. (1995). Force generation by microtubule assembly/disassembly in mitosis and related movements. Mol. Biol. Cell *6*, 1619–1640.

Jordan, M.A., Toso, R.J., Thrower, D., and Wilson, L. (1993). Mechanism of mitotic block and inhibition of cell proliferation by taxol at low concentrations. Proc. Natl. Acad. Sci. USA *90*, 9552–9556.

Maekawa, T., Leslie, R., and Kuriyama, R. (1991). Identification of a minus-end specific microtubule-associated protein located at the mitotic poles in cultured mammalian cells. Eur. J. Cell Biol. *54*, 255–267.

Margolis, R., and Wilson, L. (1981). Microtubule treadmills—possible molecular mechanism. Nature *293*, 705–711.

McIntosh, J.R. (1991). Structural and mechanical control of mitotic progression. Cold Spring Harbor Symp. Quant. Biol. *56*, 613–619.

McNally, F.J., and Vale, R.D. (1993). Identification of katanin, an ATPase that severs and disassembles stable microtubules. Cell *75*, 419–429.

McNeill, P.A., and Berns, M.W. (1981). Chromosome behavior after laser microirradiation of a single kinetochore in mitotic PtK2 cells. J. Cell Biol. *88*, 543–553.

Mitchison, T.J. (1989). Polewards microtubule flux in the mitotic spindle: evidence from photoactivation of fluorescence. J. Cell Biol. *109*, 637–652.

Mitchison, T.J., and Salmon, E.D. (1992). Poleward kinetochore fiber movement occurs during both metaphase and anaphase-A in newt lung cell mitosis. J. Cell Biol. *119*, 569–582.

Mitchison, T.J., and Sawin, K. (1990). Tubulin flux in the mitotic spindle: where does it come from, where is it going? Cell Motil. Cytoskeleton *16*, 93–98.

Moritz, M., Braunfeld, M.B., Sedat, J.W., Alberts, B., and Agard, D.A. (1995). Microtubule nucleation by γ-tubulin-containing rings in the centrosome. Nature *378*, 637–640.

Nicklas, R.B. (1977). Chromosome movement: facts and hypotheses. In: Mitosis Facts and Questions, ed. M. Little, N. Paweletz, C. Petzelt, H. Ponstingl, D. Schroeter, and H.P. Zimmermann, Berlin, Germany: Springer-Verlag, 150–155.

Nicklas, R.B., and Koch, C.A. (1969). Chromosome micromanipulation. III. Spindle fiber tension and the reorientation of mal-oriented chromosomes. J. Cell Biol. *43*, 40–50.

Rieder, C.L., and Alexander, S.P. (1990). Kinetochores are transported poleward along a single astral microtubule during chromosome attachment to the spindle. J. Cell Biol. *110*, 81–95.

Rieder, C.L., Davison, E.A., Jensen, L.C.W., Cassimeris, L., and Salmon, E.D. (1986). Oscillatory movements of mono-oriented chromosomes and their position relative to the spindle pole result from the ejection properties of the aster and half-spindle. J. Cell Biol. *103*, 581–591.

Rieder, C.L., and Hard, R. (1990). Newt lung epithelial cells: cultivation, use, and advantages for biomedical research. Int. Rev. Cytol. *122*, 153–220.

Rieder, C.L., and Salmon, E.D. (1995). Motile kinetochores and polar ejection forces dictate chromosome position on the vertebrate mitotic spindle. J. Cell Biol. *124*, 223–233.

Rieder, C.L., Schultz, A.S., Cole, R.C., and Sluder, G. (1994). Anaphase onset in vertebrate somatic cells is controlled by a checkpoint that monitors sister kinetochore attachment to the spindle. J. Cell Biol. *127*, 1301–1310.

Salmon, E.D., Inoue, T., Desai, A., and Murray, A.W. (1994). High resolution multimode digital imaging system for mitosis studies in vivo and in vitro. Biol. Bull. *187*, 231–232.

Sawin, K.E., and Mitchison, T.J. (1991). Poleward microtubule flux in mitotic spindles assembled in vitro. J. Cell Biol. *112*, 941–954.

Sawin, K.E., and Mitchison, T.J. (1994). Microtubule flux in mitosis is independent of chromosomes, centrosomes, and antiparallel microtubules. Mol. Biol. Cell *5*, 217–226.

Schiff, P.B., and Horwitz, S.B. (1980). Taxol stabilizes microtubules in mouse fibroblast cells. Proc. Natl. Acad. Sci. USA *77*, 1561–1565.

Skibbens, R.V., Rieder, C.L., and Salmon, E.D. (1995). Kinetochore motility after severing between sister centromeres using laser microsurgery: evidence that kinetochore directional instability and position is regulated by tension. J. Cell Sci. *108*, 2537–2548.

Skibbens, R.V., Skeen, V.P., and Salmon, E.D. (1993). Directional instability of kinetochore motility during chromosome congression and segregation in mitotic newt lung cells: a push–pull mechanism. J. Cell Biol. *122*, 859–875.

Vernos, I., and Karsenti, E. (1996). Motors involved in spindle assembly and chromosome segregation. Curr. Opin. Cell Biol. *8*, 4–9.

Waters, J.C., Cole, R.W., and Rieder, C.L. (1993). The force-producing mechanism for centrosome separation during spindle formation in vertebrates is intrinsic to each aster. J. Cell Biol. *122*, 361–372.

Waters, J.C., Skibbens, R.V., and Salmon, E.D. (1996). Oscillating mitotic newt lung cell kinetochores are, on average, under tension and rarely push. J. Cell Sci. (*in press*).

Wells, W.A.E. (1996). The spindle assembly checkpoint: aiming for a perfect mitosis, every time. Trends Cell Biol. *6*, 228–234.

Wilson, P.J., Forer, A., and Leggiadro, C. (1994). Evidence that kinetochore microtubules in crane-fly spermatocytes disassemble during anaphase primarily at the poleward end. J. Cell Sci. *107*, 3015–3027.

Zhai, Y., Kronebusch, P.J., and Borisy, G.G. (1995). Kinetochore microtubule dynamics and the metaphase–anaphase transition. J. Cell Biol. *131*, 721–734.

Zheng, Y., Wong, M.L., Alberts, B., and Mitchison, T. (1995). Nucleation of microtubule assembly by a γ-tubulin-containing ring complex. Nature *378*, 578–583.